ME 563:
Nonlinear
Finite Element
Analysis

Spring | 2016

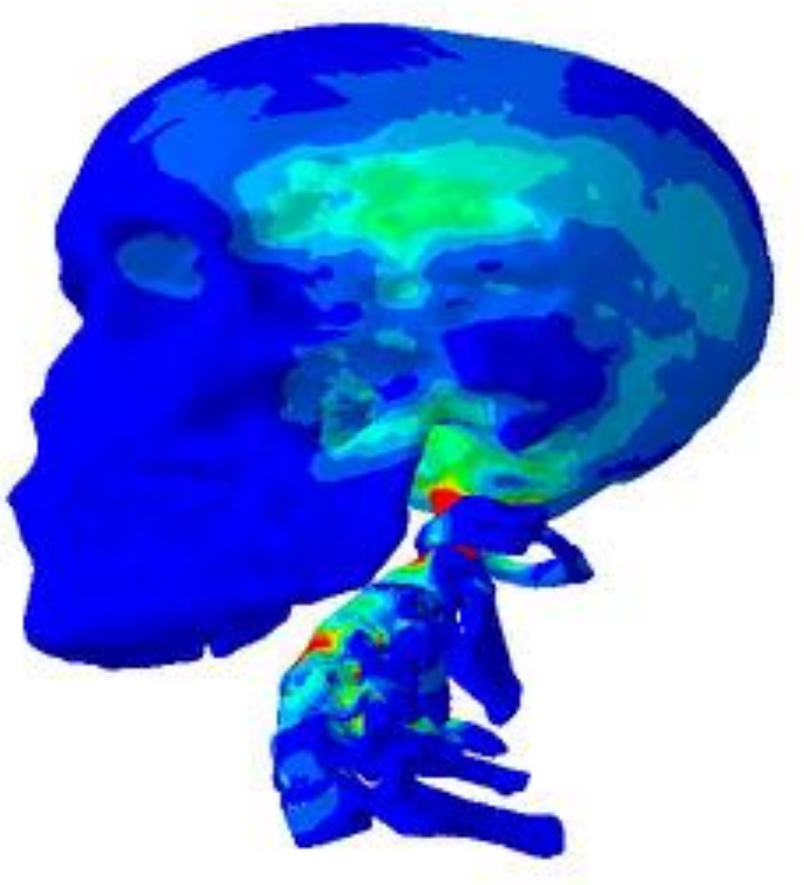

The Development and Analysis of a Finite Element Model of the C45 Cervical Spine Segment

Group Members:

Vikram Subramani, Jones Justin

PennState
College of Engineering

Department of Mechanical and Nuclear Engineering, University Park, PA

Table of Contents

Executive Summary

Injury to the human cervical spine is a major cause for concern in the industrialized world. In the sports industry, there are many cases of spinal injury resulting from high magnitude frontal impacts to the head. Automobile accidents are another common cause for spinal injury. Apart from the high magnitude impact loading scenarios described above, fatigue loading is also another major cause for damage to the cervical spine, especially the intervertebral discs. This type of fatigue damage is commonly seen in the military because military personnel are required to wear heavy helmets and head-supported gear on a daily basis. It has been established that degeneration of the intervertebral discs is the primary cause of neck pain. Therefore, it is essential to study the biomechanics of the cervical spine, in order to understand the mechanism of damage propagation in the spine, especially the intervertebral discs.

Before attempting to build a model of the entire head and cervical spine assembly, we propose to develop a finite element model of the C45 spinal segment. This comprises of the C4 vertebra, C5 vertebra and the C45 intervertebral disc. After developing the model, we will attempt to validate the kinematics of the model against existing experimental data, for flexion/extension and compression/tension loading. We will run these simulations in ABAQUS, using Penn State's Lion-XV and Lion-XG clusters. The results of the validation simulations will be analyzed and the model will be improved in such a way that the model response matches the experimental data.

As a meshing exercise, we have also developed a tetrahedral element mesh of the atlas bone of the cervical spine. The geometry file for this bone was imported from BodyParts3D, which is an open-source anatomical database of an adult human male offered by The University of Tokyo (Mitsuhashi et al., 2009). This geometry file was imported into MeshLab, which is the meshing software in which the tetrahedral mesh was developed.

Acknowledgements

We would like to thank Dr. Reuben Kraft, Shuman Assistant Professor of Mechanical Engineering at Penn State University for the opportunity to work on this project. His guidance has provided us with the required background knowledge of ABAQUS, and he has graciously allowed us to use the computational resources available through the Computational Biomechanics Lab at Penn State for running simulations for our project.

We would also like to thank Radha Krishna, Garimella Harsha Teja and Shruti Motiwale from the Computational Biomechanics Group at Penn State for their invaluable input on correcting various issues with the model and getting the model running properly.

List of Figures

Section 1: Background and Project Plan

The cervical spine is one of the critical injury regions of the human body in a variety of scenarios. The majority of all spinal injuries are caused by automobile accidents, in which the cervical spine is the primary injury site. Moreover, frontal impact to the head leading to cervical spine injury is a very common issue in the sports industry. Therefore, studying the effects of various types of loading on the head on the injury mechanisms at play in the cervical spine is of prime interest in the field of safety in the automobile industry and the sports industry. Apart from the high magnitude impact loading scenarios described above, fatigue loading is also another major cause for damage to the cervical spine, especially the intervertebral discs. This type of fatigue damage is commonly seen in the military because military personnel are required to wear heavy helmets and head-supported gear on a daily basis. This exposes their cervical spines to complex cyclic loading over long periods of time. It has been established that severe neck pain resulting from degeneration of the intervertebral discs in the cervical spine is a major cause for evacuation of soldiers from military service. Therefore, it is essential to study the biomechanics of the cervical spine, in order to understand the mechanism of damage progression in the spine.

One of the methods used to assess vehicle safety in the automobile industry is crash testing involving the actual crash of a vehicle in a controlled environment, with an anthropometric dummy seated inside it. The test dummy has sensors embedded in it which are used to measure the occupant response to the crash impact load. However, this is a very expensive and destructive process which cannot be repeated in an unlimited fashion. Due to the high cost of crash testing, it becomes necessary to turn to computational numerical modeling to fully understand the effect of impact loading on the human cervical spine.

The first step in the project was to obtain accurate geometry and develop finite element meshes of the C4 vertebra, C5 vertebra and the C45 intervertebral disc. We obtained the geometry files for meshing from BodyParts3D, which is an open-source anatomical database of an adult human male offered by The University of Tokyo (Mitsuhashi et al., 2009). This geometry was imported in to ANSYS ICEMCFD and meshed together. Also, as further practice of the meshing process, we meshed the atlas bone of the cervical spine using Meshlabs, which is an open source meshing software. Details of the meshing process have been provided in the Mesh Development section of this report.

The next step involved setting up the flexion/extension and compression/tension simulations using ABAQUS. The material properties for the different components of the model were obtained from literature and assigned to various regions of the C45 segment. After assembling the model, the boundary conditions were specified which hold the inferior surface of the C5 vertebral body fixed. After this, the flexion/extension moment or the compression/tension load was applied to the superior surface of the C4 vertebral body. General contact was defined for the model which prevents surfaces from penetrating each other. The simulations were submitted using the Static General solver in ABAQUS. The extent of the C45 segment motion was recorded for varying magnitudes of loading, and the results were compared against existing experimental data.

As a final effort, we have investigated ways to improve the biofidelity of the model in order to obtain a better match between the model response and the experimental data. The changes we made in order to achieve this have been outlined in the following paragraphs.

We added spinal ligaments to the finite element model. Ligaments are an important component of the cervical spine, playing a significant role in governing the kinematics of spinal segment motion. Ligaments provide tensile force under extension, which has a restrictive effect on relative motion between the two vertebrae of the spinal segment.

In our initial model, the intervertebral disc was modelled as a single homogeneous material. However, in reality the intervertebral disc is divided into two distinct regions: the central nucleus pulposus and the surrounding annulus fibrosus. Therefore, we developed a segmented mesh of the intervertebral disc, which captures this segmentation into the nucleus and annulus. This will enable us to assign appropriate material properties separately to the nucleus region and annulus region, which are significantly different.

Finally, the validation simulations were repeated on this improved model. The response of the initial model (without ligaments and segmented disc) was compared against the response of the improved model (with ligaments and segmented disc) and these results were compared against the experimental data. We then present our major results and findings before concluding the report.

Section 2: Development and Description of the CAD Geometry

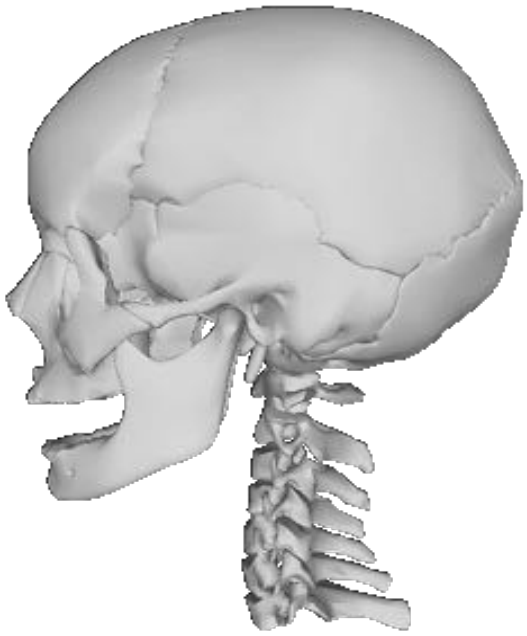

Figure1: CAD Geometry of Human Skull and cervical spine**.**

Unlike mechanical components that have relatively simple geometries and dimensions that can be easily obtained online from websites like McMaster Carr, human anatomy is made up of many complex systems with unique geometries. Further, this unique geometry can be very different between separate individuals. Do to these inherent complexities the CAD geometry of anatomy is extraordinarily difficult to create and similarly difficult to come by.

Since the human skull and cervical spine are a highly complex system composed of many bones, ligaments, and muscular tissue the task to track down CAD files is daunting. However, there are several for pay sites that offer wide varieties of models, such as 3DScience or Pacific research Labs, but typically these can cost hundreds or thousands of dollars for the CAD files. Due to the financial restrictions of this project these options are not feasible and an open source CAD repository had to be used.

The CAD for our model came from the geometry available on BodyParts3D, which is an open-source anatomical database of an adult human male offered by The University of Tokyo (Mitsuhashi et al., 2009). To reduce computational costs as much as possible the final CAD geometry that was used for this report only included the C4-C5 and intervertebral segments, but an anatomically correct cervical spine and skull can be seen in Figure 1.

If the time and resources were available and it was completely necessary to create CAD geometry of the human skull and cervical spine, or any human anatomy for that matter, digital imaging such as MRI or CT could be used. The stack images could then be used in an algorithm that segment each layer by selecting the boundary of the parts of interest, than combine them into a 3D surface. Once the parts of interest are segmented, polygonal surfaces may be generated. This can be done by stitching together stacks of closed bounded contours. This will result in the desired 3D CAD geometry that can then be meshed and used for FEM.

Researchers have investigated the geometry and dimensions of the vertebrae and intervertebral discs in the cervical spine experimentally. Measurements were performed on the geometry surface files of the C4 vertebra, C5 vertebra and the C45 intervertebral disc obtained from BodyParts3D. These measurements were compared to the cervical spine measurements done in a morphometric study by Bazaldua *et al.* [7] on a Mexican population. Figure 2 shows a sectional view of the C4

vertebra which depicts the exact manner in which the length and width of the vertebrae were measured in the study [7].

Given below in Table 1 is a comparison between the dimensions of the C4 and C5 vertebrae measured experimentally against the measurements made on the geometry files from BodyParts3D. It can be seen that the model dimensions closely matched the experimental measurements.

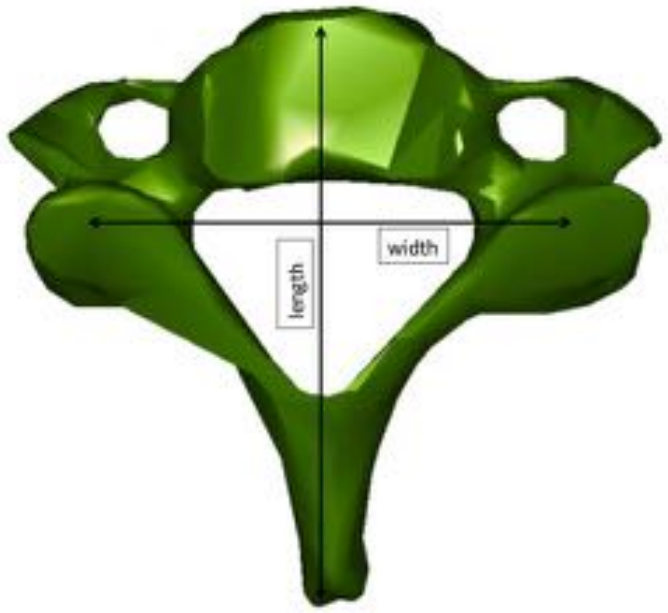

Figure 2: Sectional view of the C4 vertebra depicting length and width measurements

Table 1: Comparison between model dimensions and experimentally measured dimensions of the C4 and C5 vertebrae

Vertebra Level	Model length	Mean length from experiment	Model width	Mean width from experiment
C4	49.5 mm	52.3 mm	39.4 mm	43.4 mm
C5	53.7 mm	53.6 mm	42.5 mm	46.3 mm

Section 3: Development of Finite Element Meshes

The intervertebral disc is divided into two distinct regions: the central nucleus pulposus and the surrounding annulus fibrosus. The nucleus pulposus is composed of a soft, incompressible material, which behaves like a fluid. The annulus fibrosus region is densely packed with collagen fibers, which preserve the structural integrity of the disc. Therefore, it is essential to develop a mesh of the intervertebral disc, which captures this segmentation into the nucleus and annulus. This will enable us to assign appropriate material properties separately to the nucleus region and annulus region, which are significantly different.

We have created a tetrahedral mesh for the C45 spinal segment, which consists of the C4 vertebra, C5 vertebra and the C45 intervertebral disc. We have developed a segmented mesh of the C45 intervertebral disc, which will be incorporated into the finite element model along with the vertebrae. The nucleus and annulus are arranged as concentric layers, i.e. their outlines have the same shape. Therefore, to obtain the segmented mesh, the geometry of the whole disc was first imported into Blender. This surface was copied and shrunk in such a way that the shrunk surface represented the outline of the nucleus. This shrunk surface was concentrically embedded in the original disc surface and extruded on both sides, as shown in Figure 3.

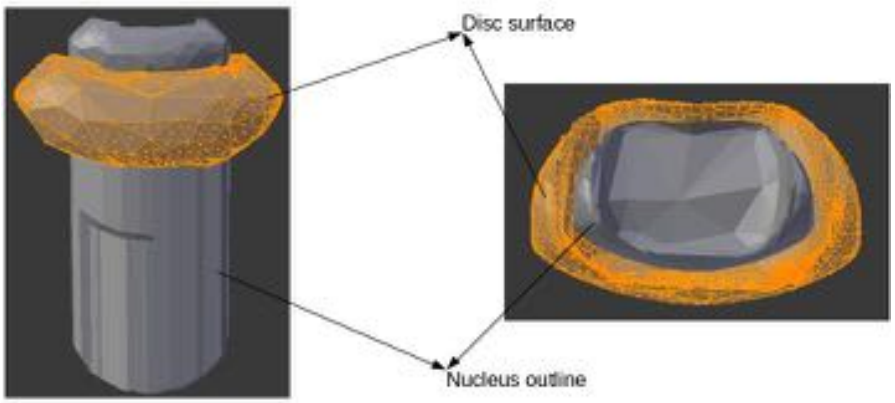

Figure 3: Process of embedding the geometry of the disc within itself in Blender to create a surface for the nucleus pulposus

These surfaces were then exported into ANSYS ICEMCFD. The automatic meshing algorithm in ICEMCFD was used to create a volume mesh with tetrahedral elements of the surfaces shown in Figure 1. The meshing algorithm in ICEMCFD automatically segmented this volume mesh into 4 regions: the desired nucleus and annulus regions of the disc, and the 2 undesired extrusions. These extrusions could simply be deleted in order to obtain the segmented mesh of the intervertebral disc shown in Figure 4.

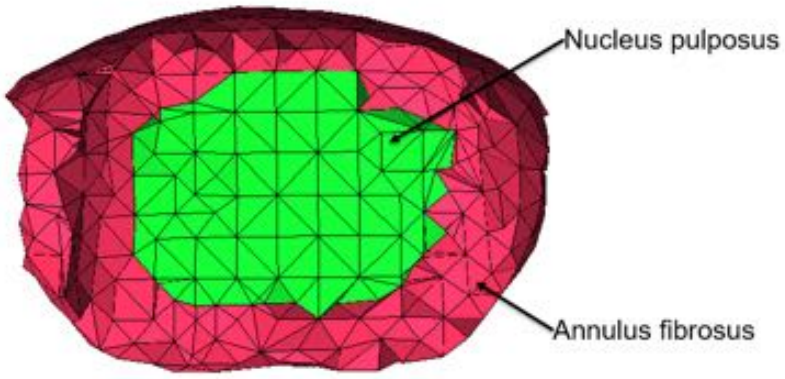

Figure 4: Segmented mesh of the C45 intervertebral disc

After obtaining a segmented mesh of the intervertebral disc, separate surface files for the nucleus and annulus were created. These new surface files were imported into ANSYS ICEMCFD along with the surface files for the C4 vertebra and C5 vertebra. The entire geometry was meshed with tetrahedral elements using the automatic meshing algorithm in ICEMCFD. The resulting mesh of the C45 segment contained 34327 tetrahedral elements. The meshing algorithm automatically defined shared nodes at the interfaces between the vertebrae and the intervertebral disc. This mesh has been shown in Figure 4, along with a zoomed view of the interface between the vertebrae and the intervertebral disc.

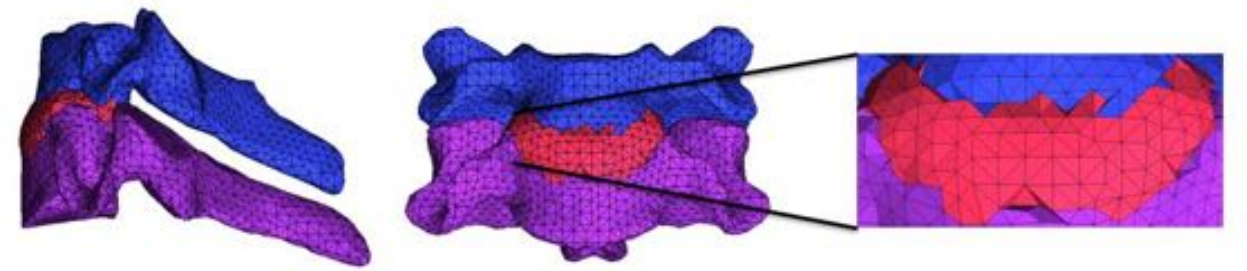

Figure 5: Side view (left) and front view (middle) of the C45 segment mesh, along with a zoomed view of the interface between the disc and vertebrae (right)

This mesh was then exported into ABAQUS and the ligaments were added to the model in the form of truss elements. Ligaments are an important structural component of the cervical spine. Spinal ligaments are tissues that connect vertebrae to adjacent vertebrae in the spinal column. Under various modes of physiological loading, ligaments tend to dampen relative motion between vertebrae because they provide a tensile force under elongation.

Care was taken to specify that the ligaments do not support compressive loads, by selecting the 'No Compression' option for the truss elements. The truss elements were placed in the appropriate regions on the vertebrae, with one of the nodes tied to a node on the C4 vertebra and the other node tied to a node on the C5 vertebra. The three different classes of cervical spine ligaments used in

the model (capsulary ligaments, intertransverse ligaments and interspinous ligaments) have been shown in Figure 6.

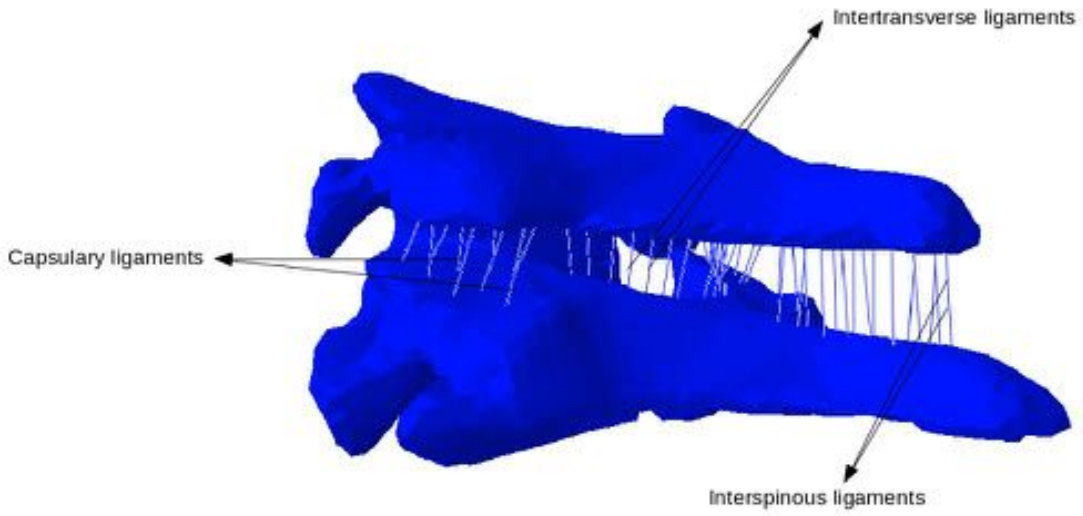

Figure 6: Classes of ligaments added to the C45 finite element model

This complete mesh was used to run our flexion/extension and compression/tension validation simulations.

Section 4: Development and Description of the Model Assembly and Boundary Conditions

As mentioned previously, the entire geometry was meshed together in ANSYS ICEMCFD and shared nodes were automatically defined at the interface between the vertebrae and the intervertebral disc. Since the relative positions of the vertebrae and intervertebral disc with respect to one another was already anatomically correct, we did not have to manually connect various components of the mesh together. The only additional features we had to incorporate with the C45 segment mesh imported from ICEMCFD were the ligaments, which were modelled as truss elements in ABAQUS. The cross sectional area of these ligaments was taken to be 1 square millimeter. One node of each of the ligaments was connected to a node on the inferior surface of the C4 vertebra, and the other node of each ligament was connected to a node on the superior surface of the C5 vertebra. Now that we had the model assembly all set up, we assigned material properties to the various components of the C45 segment model.

The vertebrae were both modeled as linear elastic materials. Both the annulus and nucleus of the intervertebral disc were modelled as Mooney-Rivlin hyperelastic materials (with different coefficients). The ligaments were modelled with linear elastic material. Care was taken to specify that the ligaments do not support compressive loads, by selecting the 'No Compression' option for the truss elements used to model the ligaments. Table 2 provides details on the material models assigned to different regions of the C45 segment.

Table 2: Material properties for the C45 model.

Linear Elastic Material				
Component	**Density**	**Elastic Modulus**	**Poisson's Ratio**	
Vertebrae	1900 kg/m^3	12 GPa	0.3	
Ligaments	1000 kg/m^3	5 MPa	0.4	
Hyperelastic Material				
Component	**Density**	**C1**	**C2**	**D**
Annulus Fibrosus	300 kg/m^3	0.56 MPa	0.14 MPa	0.143
Nucleus Pulposus	1000 kg/m^3	0.12 MPa	0.03 MPa	0.067

After assigning material properties, we set up the boundary conditions for our flexion/extension and compression/tension validation simulations. The flexion/extension simulation results were validated against the cervical spine flexion/tension experiments of Nightingale *et al.* (2007). The

compression/tension simulation results were validated against the compression/tension experiments of Panjabi *et al.* (1986) and Dibb *et al.* (2009).

In order to simulate the experimental conditions, the inferior end of the C5 vertebral body was held fixed while the required load was applied to a node on the superior surface of the C4 vertebral body. The fixed nodes and the nodes on which the loading is applied has been shown below in Figure 7.

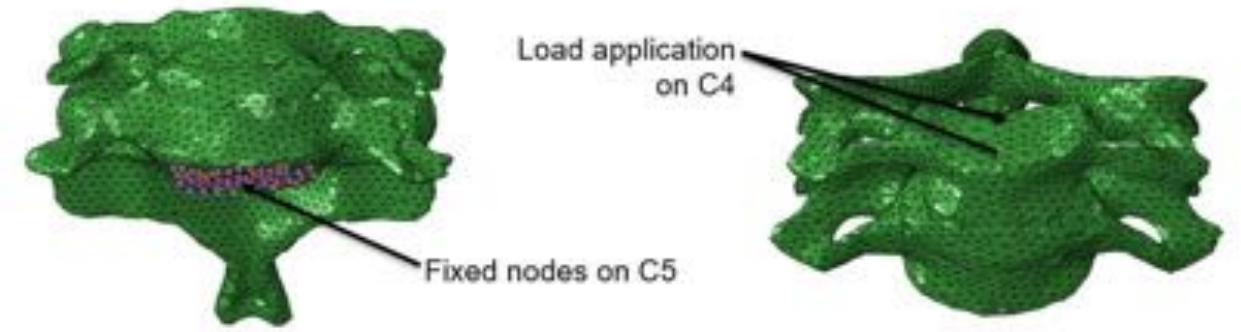

Figure 7: Fixed nodes on the lower surface of C5 (left) are shown by the orange/blue dots. The nodes on which the load is applied (right) are shown by the small yellow arrows on the upper surface of C4

Simulations were run for flexion/extension loads of varying magnitudes, beginning at 0.25 N-m and increasing in steps of 0.25 N-m up till 1.5 N-m. The resulting rotation angle of the C4-C5 joint was measured and the results were compared with the above mentioned experimental data. Simulations were also run for compression/tension loading. Using the experimental results from Panjabi *et al.*, the compressive load was set to 100 N in the negative z direction. As for the tension validation the load was set to 500 N in the positive z direction in accordance with the experiments of Dibb *et al*. The rate of loading was not explored in this validation. The results of the validation simulations have been presented in a later section.

Section 5: Development and Description of Model Interactions

As mentioned previously the mesh developed in ICEMCFD was exported to ABAQUS. The FEA model interactions used in ABAQUS was general contact with the contact domain surface pairs "All* with self" selected. The interaction properties used frictionless tangential behavior.

Using the built in general contact algorithm to model contact allows for the contact between the segments to be defined with a single interaction that is then applied to all the bodies of the model. Doing this ensures that there is no penetration of elements throughout the model by utilizing a penalty method for contact. Frictionless tangential behavior for the interaction properties was used for simplification and to reduce computational cost.

For the second validation simulation the same loading conditions were applied but the model included ligaments and a segmented intervertebral disk ligaments. New constraints had to be created for the ligaments. This was accomplished by tie constraining between the ligament parts (slave) and the corresponding vertebra body (master) and can be seen in Figures 8 and 9.

Figure 8: Highlighted ligament slave tie nodes. The end nodes of each ligament were tied to their corresponding master node on the vertebra body

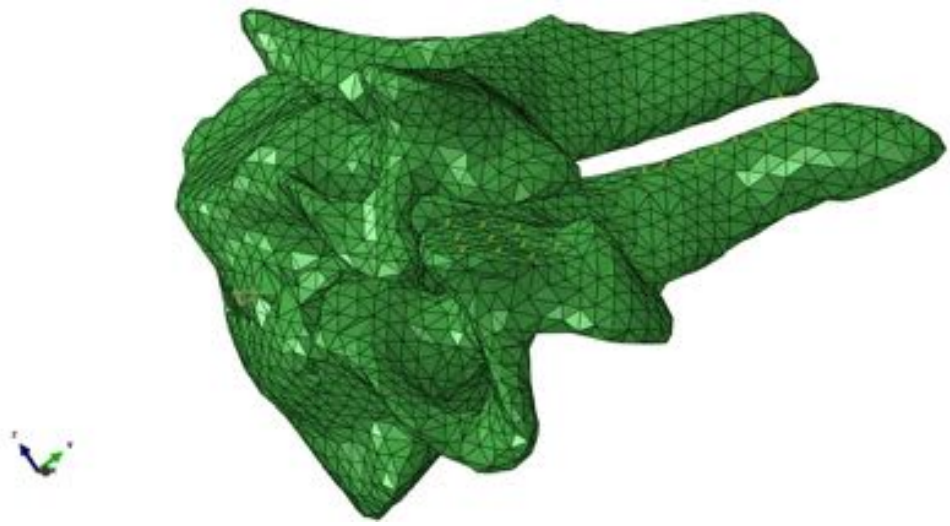

Figure 9: Highlighted Vertebra master tie nodes. Each highlighted node of the vertebra body was tied to their corresponding ligament slave node.

Section 6: Analysis of Finite Element Model

The simulations of the C45 model were run using the 'Static-General' step type in ABAQUS. This step type was chosen because the experiments against which we are validating our results were performed in quasi-static conditions, and the 'Static-General' step is a good choice to simulate quasi-static processes.

For the full skull and cervical spine model it is intended that the simulation will use the step type of 'Dynamic-Implicit' since the effects of frontal impacts will be a highly nonlinear problem. However, dynamic implicit modeling updates the stiffness matrix after every increment and requires very small increments to be accurate and thus is computationally taxing. This is another reason that the static general step was also chosen for the C45 validation model. Whereas a dynamic implicit model may take several hours to solve, the static general model of the C45 took approximately 15 minutes to solve.

In order to ascertain whether the model would be able to take advantage of parallel processing the simplified C4-C5 model was ran in a compressive simulation with a point load of 2500N. This loading scenario was ran three times with 1, 2, 4, 8, 12, 14, and 16 processors in order to determine the models scalability. The wall time and the CPU time was recorded in seconds for analysis. The model is seen to benefit from parallel processing as seen in figure 10.

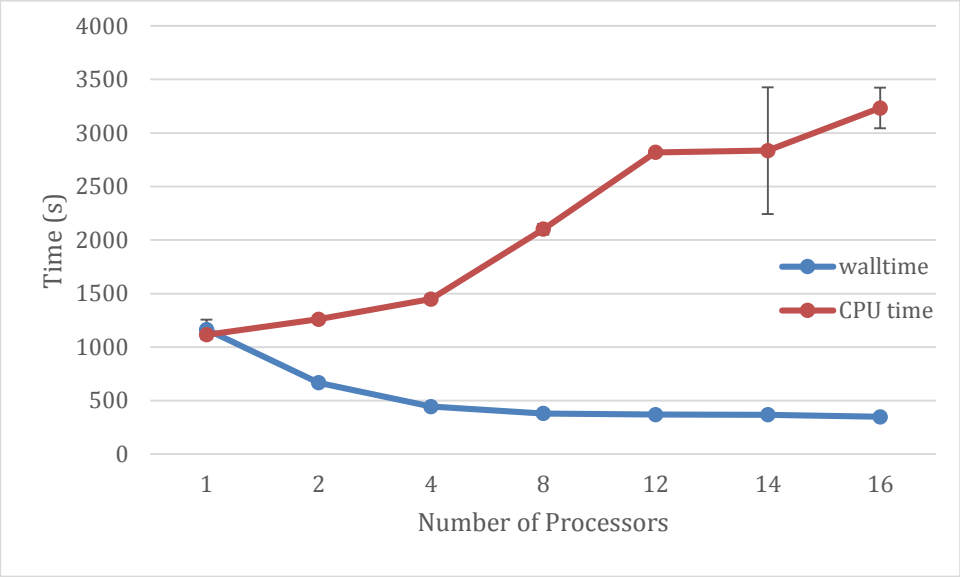

Figure 10: Parallel processing sensitivity analysis of the C45 simulation

The largest benefit is gained from one to two processors with a reduction in wall time of 497 seconds. Going from two to four processors gives another reduction of 223 seconds of wall time. After this there is a much smaller increase in wall time and a large increase in CPU time and may not be beneficial depending on the system

Section 7: Summary of Major Findings

Results of Initial Model (without ligaments and segmented disc):

First, we present the results for the flexion/extension and compression/tension simulations run on the initial model. The flexion/extension results of the initial model have been shown in Figure 11 and Figure 12, which allow for easy comparison between the experimental data and simulation results.

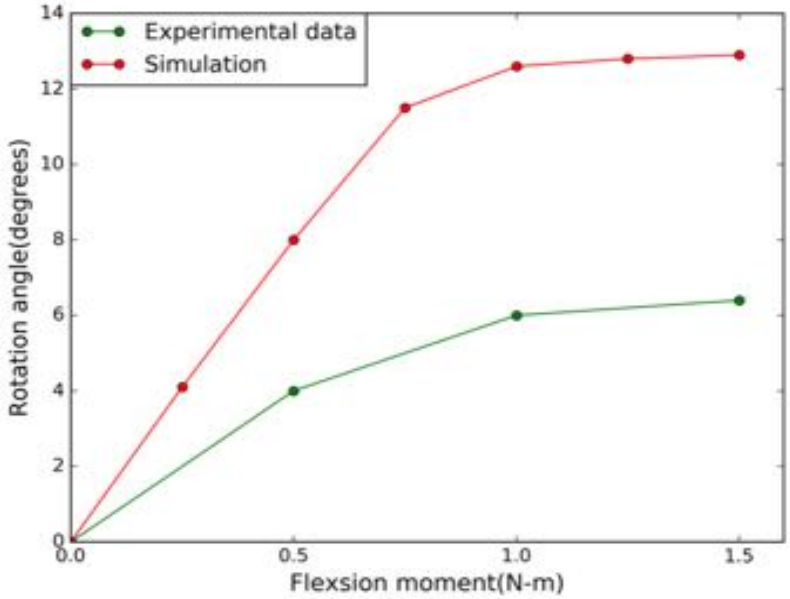

Figure 11: Comparison of experimental data and simulation results for flexion loading of the C45 segment

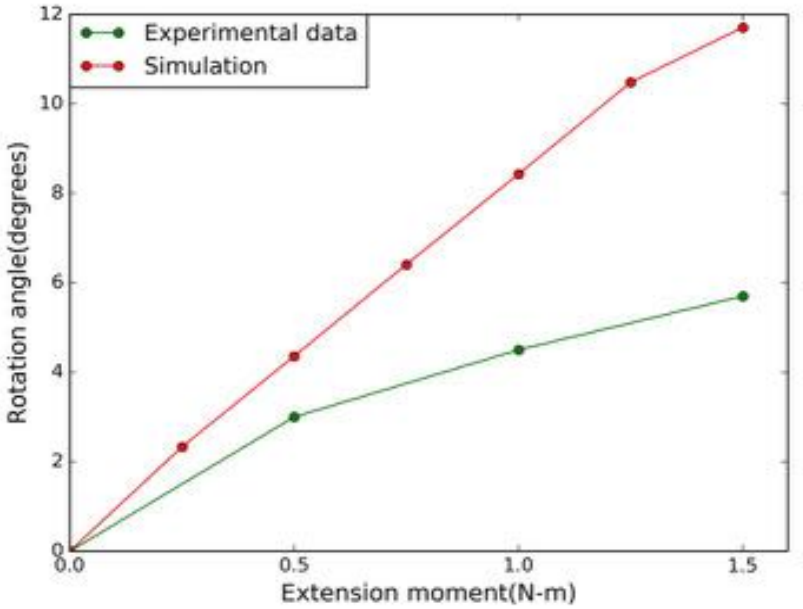

Figure12: Comparison of experimental data and simulation results for extension loading of the C45 segment

The results for tensile loading conditions can be seen in Table 3 as well as Figure 13. The simulated stiffness was 42% of the experimental results. From Figure 13 it can be seen that the relationship between applied force and displacement is approximately a linear relationship, which is not seen in the experimental results. The peak displacement for the simulation was 1.17mm at 233N compared to the 0.8mm at 300N seen in the experiment. Even though a 500N force was used the max load of the simulation was 233N due to the simulation aborting.

Table 3: Tensile stiffness validation

	Stiffness (N/mm)	Peak Displacement
Dibb *et al.* (2009)	438.8 ± 98.6	0.8 ± 0.2
Simulation	185.0 ± 3.46	1.17

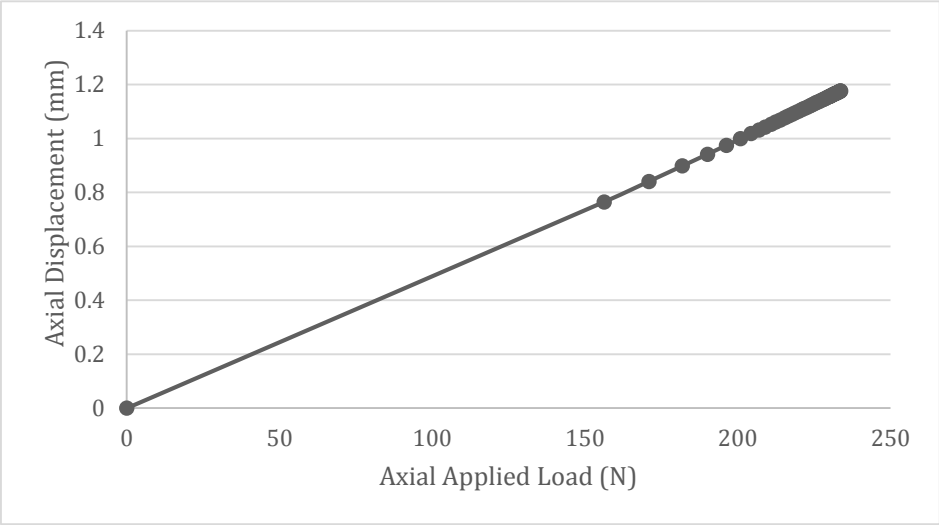

Figure13: Axial displacement (mm) of the C45 segment model versus the applied axial tensile load (N).

As for the compressive loading scenario the force in the z direction versus displacement can be seen in Figure 14 well as Table 4. Table 4 shows that the simulation model was only 67% as stiff as the experimental results in compression. However, from Figure 14 the simulation seems to be stiffer than the experimental data. This discrepancy is most likely a result of the large standard deviation of the experimental data. In Figure 14 the compressive stiffness is seen to be linear in both the simulation and the experiment, however only one point of data was available for the experimental data so this may not necessarily be the case.

Table 4: Compressive stiffness comparison between experimental results and simulation. Note the large SD of the experimental data

	Stiffness (N/mm)
Panjabi et al (1986)	338 ± 399.9
Simulation	226.9 ± 7.32

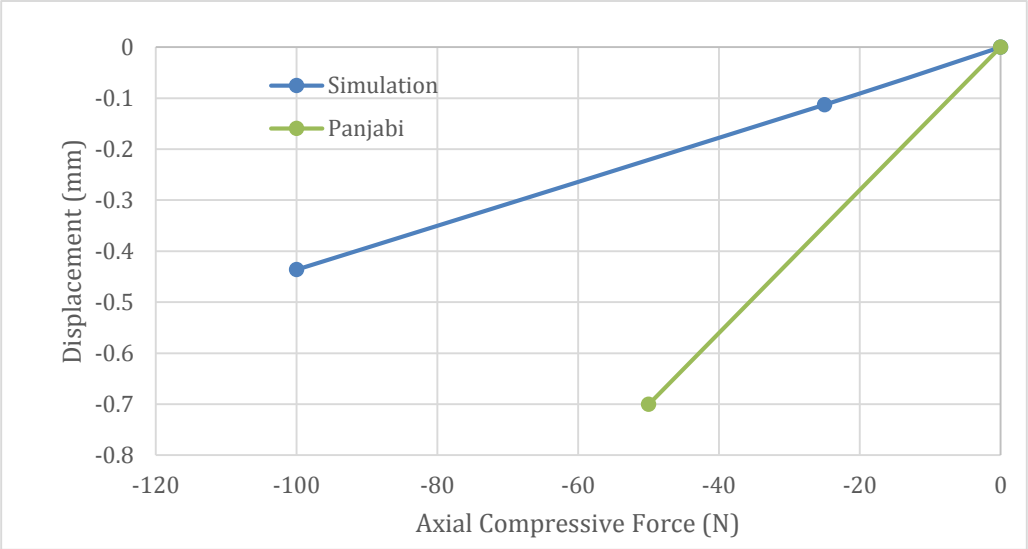

Figure14: Axial displacement (mm) of the C45 segment model versus the applied axial compressive load (N), compared against the experimental data of Panjabi *et al.*

From these results, it can be seen that the simulation results for extension loading are more compliant with the experimental data as compared to the results for flexion loading. Also, it is quite clear that the simulation results in both the cases of flexion and extension tend to show an angle of rotation significantly greater than the experimental readings. This discrepancy may be due to the absence of ligaments in the initial model. The ligaments can be expected to have sufficient tension to restrict the joint rotation, thus reducing the angle of rotation for a particular load. Therefore, addition of ligaments to the model is a necessary step that will make the model more bio-fidelic and bring the simulation results closer to the experimental data.

The simulation results of compression and tension are more compliant than what was seen in the experimental results. It was also shown that the relationship between the force and displacement of the segment is linear, which is not what was typically seen in the experimental case. Further, if the loads are increased past relatively small loads, above 300N, the simulation aborts prematurely.

Results of Final Model (with ligaments and segmented disc):

Only flexion simulations were run on the final model due to the limited timeline of this project. Figure 15 shows the variation of joint rotation angle with flexion moment for the experimental data, the model without ligaments and the model with ligaments.

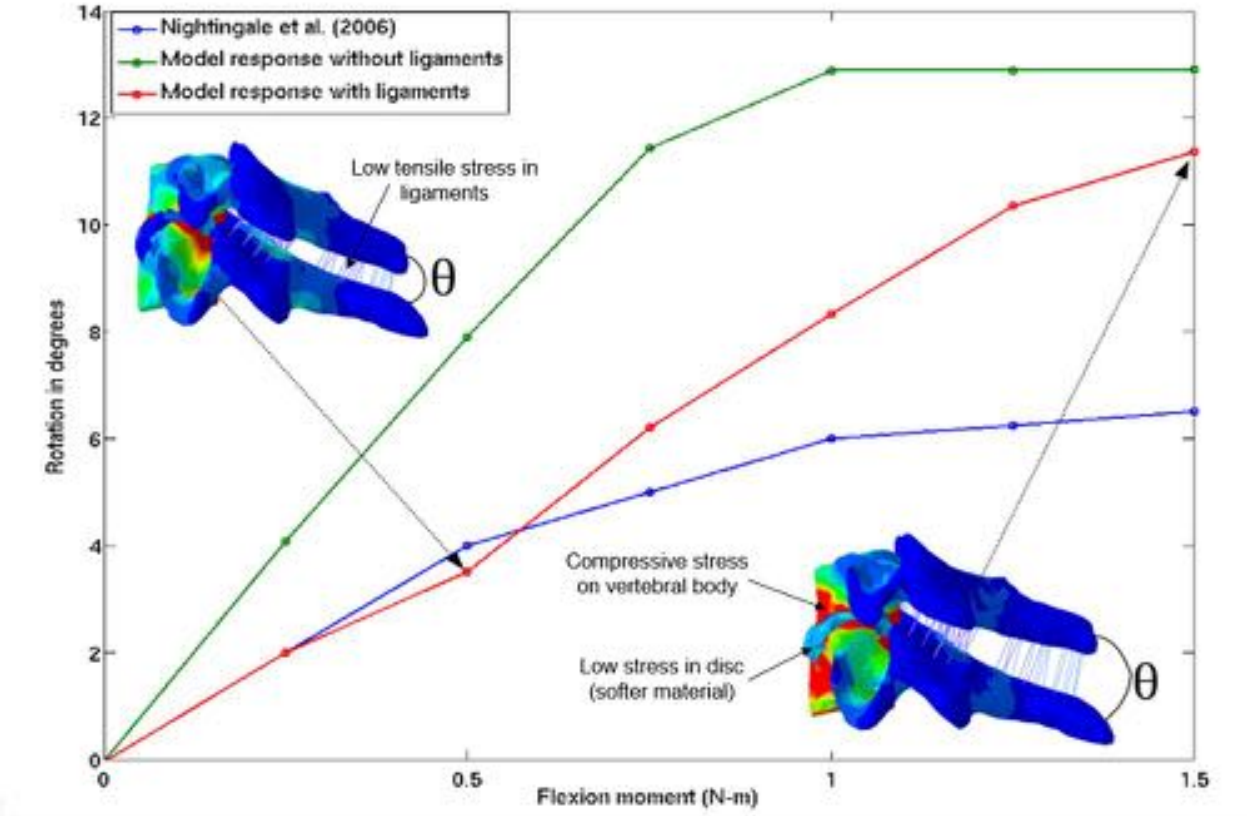

Figure 15: Comparison of experimental data and simulation results for flexion loading of the C45 segment

From Figure 15, it is clear that the model without the ligaments undergoes a much larger angle of rotation compared to the experimental results. As expected, the model with the ligaments has a lower angle of rotation than the model without the ligaments, and is much closer to the experimental data. This can be attributed to the restrictive action of ligament tension on joint rotation.

However, the response of the model with ligaments also diverges away from the experimental data for higher loads (>1 N-m). To address this discrepancy, the use of a non-linear material model for the ligaments will be investigated, which will be aimed at increasing the elastic modulus of the ligaments at large strains.

Future Work and Areas for Improvement:

- Apply non-linear elastic properties to the ligaments.
- Obtain a smoother geometry for the disc and re-mesh to improve the disc-vertebra interface.
- Model the facet joints between the vertebrae.
- Perform similar validation for the C34 segment.

Section 8: References

[1] van den Oord, Marieke HAH, et al. "Neck pain in military helicopter pilots: prevalence and associated factors." *Military medicine* 175.1 (2010): 55-60.

[2] Qasim, Muhammad, et al. "Initiation and progression of mechanical damage in the intervertebral disc under cyclic loading using continuum damage mechanics methodology: a finite element study." *Journal of biomechanics*45.11 (2012): 1934-1940.

[3] Makwana, Anand R., et al. "Towards a Micromechanical Model of Intervertebral Disc Degeneration Under Cyclic Loading." *ASME 2014 International Mechanical Engineering Congress and Exposition*. American Society of Mechanical Engineers, 2014.

[4] DeWit, Jennifer A., and Duane S. Cronin. "Cervical spine segment finite element model for traumatic injury prediction." *Journal of the mechanical behavior of biomedical materials* 10 (2012): 138-150.

[5] Panzer, Matthew. "Numerical modelling of the human cervical spine in frontal impact." (2006).

[6] Weiss, Jeffrey A., et al. "Three-dimensional finite element modeling of ligaments: technical aspects." *Medical engineering & physics* 27.10 (2005): 845-861.

[7] Bazaldua, C. J. J., et al. "Morphometric study of cervical vertebrae C3-C7 in a population from northeastern Mexico." *Int. J. Morphol* 29.2 (2011): 325-330.

[8] Nightingale, Roger W., et al. "Flexion and extension structural properties and strengths for male cervical spine segments." *Journal of biomechanics* 40.3 (2007): 535-542.

[9] Panjabi, Manohar M., et al. "Three-dimensional load-displacement curves due to froces on the cervical spine." *Journal of orthopedic research* 4.2 (1986): 152-161.

[10] Dibb, Alan T., et al. "Tension and combined tension-extension structural response and tolerance properties of the human male ligamentous cervical spine." *Journal of biomechanical engineering* 131.8 (2009): 081008.

[11] Zhou, Xianlian, Phillip Whitley, and Andrzej Przekwas. "A musculoskeletal fatigue model for prediction of aviator neck maneuvering loadings. *"International Journal of Human Factors Modelling and Simulation 2* 4.3-4 (2014): 191-219.

[12] Adams, Michael A., and Peter J. Roughley. "What is intervertebral disc degeneration, and what causes it?." *Spine* 31.18 (2006): 2151-2161.

[13] Panzer, Matthew B., and Duane S. Cronin. "C4–C5 segment finite element model development, validation, and load-sharing investigation." *Journal of biomechanics* 42.4 (2009): 480-490.

[14] Chazal, J., et al. "Biomechanical properties of spinal ligaments and a histological study of the supraspinal ligament in traction." *Journal of biomechanics* 18.3 (1985): 167-176.

[15] Panjabi, Manohar M., Thomas R. Oxland, and Edward H. Parks. "Quantitative anatomy of cervical spine ligaments. Part II. Middle and lower cervical spine." *Journal of Spinal Disorders & Techniques* 4.3 (1991): 277-285.

[16] Yoganandan, Narayan, Srirangam Kumaresan, and Frank A. Pintar. "Geometric and mechanical properties of human cervical spine ligaments."*Journal of biomechanical engineering* 122.6 (2000): 623-629.